A Cyclic Compartmental Model Approach to the Nemesis of Consciousness: Alzheimer's

Helme Castro[1], Sunhwa Choi[2], Natalia Rodríguez[3], YuJie Shui[4], Joaquín Rivera[5], David Tello[5], Griselle Torres-García[5], Abdessamad Tridane[5]

[1]School of Materials, Arizona State University, Tempe, AZ 85281
[2]Department of Mathematics, Konkuk University, Seoul, Korea 143-701
[3]Departamento de Matemática-Física, Universidad de Puerto Rico-Cayey, PR 00736
[4]Department of Biomedical Engineering, Boston University, Boston, MA 02215
[5]Department of Mathematics and Statistics, Arizona State University, Tempe, AZ 85281-1804

Abstract

Whether researchers favor the physiological or psychological approach, the agreement remains, Alzheimer's disease (AD), is the enemy of consciousness, especially that of elders. Intense research has been done, yet, scientists have not discovered a successful method to prevent AD's inevitable neurodegenerative progression. However, recent research discovered that rats have acquired certain AD symptoms upon the injection of Amyloid-beta-42 ($A\beta_{42}$) protein. While Amyloid beta protein has always been a theory to Alzheimer's cause, researchers were unable to distinguish whether this protein is a cause or a symptom until this discovery. With this result, our research suggests that $A\beta_{42}$ is one of the puzzling reasons for AD. Particularly, the input and output around $A\beta_{42}$ will be the basis of this mathematical modeling approach. For our purposes, the modeling proposal follows a continuous cycle observed solely through AD patients. Building on the work of Reed et al. (2002), our aim is to describe the fundamental aspects of this common cycle among Alzheimer's patients and then propose a qualitative initiation of AD. With an emphasis on the dynamics of methionine and homocysteine in Reed's Methionine Cycle, we monitor the qualitative decrease of $A\beta_{42}$ level to determine the progression of AD.

A Introduction

When Alois Alzheimer discovered this disease a century ago in 1907, Alzheimer's disease (AD) immediately became the prevalent fear for elders. According to a 2008 National Center for Statistics survey, AD is the seventh leading source of death in the United States, causing 71,559 deaths each year [31]. In perspective with other leading causes of death such as heart failure or cancer, AD is one of only two diseases (Parkinson's being the other) to show an incline, demonstrating the society's vulnerability to prevent, let alone cure, the disease [31]. In fact, this deadly type of dementia is neither proven infectious nor genetic, and the only visible trend is the number of incidences rises as people age with the favorable initial onset at age 65, based on a few exceptions [1].

From the simplest anatomical description, AD starts with initial damage to nerve cells in the entorhinal cortex and eventually ends with the obliteration of the hippocampus, all of which occurs in brain's temporal lobe, a region crucial to cognitive functions [26]. In relations to AD's severity, the amount and distribution of neurofibrillary tangles (protein aggregates found within neurons) within the cerebral cortex, dictates the intensity of symptoms. According to the Alzheimer Association, the disease is divided into seven stages, with a progressive pattern of cognitive and functional impairment expressed during each stage: (I) No impairment (pre-diagnosis), (II) Very mild decline, (III) Mild decline, (IV) Moderate decline (mild or early stage), (V) Moderate severe

decline (moderate or mid-stage), (VI) Severe decline (moderately severe or mid-stage) and (VII) Very severe decline (severe or late stage) [1]. People in the early stages of AD may experience lapses and word confusion. As the disease progresses, patients will experience memory loss, personality changes, daily life disabilities, and eventually death. People with AD die after an average of four to six years after diagnosis; however, the disease can last from three to twenty years [1]. For the purpose of this work, we simplified the disease into only three stages: mild, moderate, and severe.

Biologically, recent research from Harvard Medical School demonstrates that a particular form of Amyloid beta($A\beta$) protein plays a fundamental role in AD [12]. $A\beta$ is a peptide of 39 to 43 chain of amino acids, with $A\beta_{40}$ and $A\beta_{42}$ as the most common forms [22]. Generally, the protein arises from enzymatic cleavage of a larger amino acid precursor protein (APP), processing both amyloidogenic ($A\beta$) and non-amyloidogenic products. In contrast to the normal α-secretase cleavage into the less accumulative (likely to polymerize) $A\beta_{40}$, AD patients suffer from the β-secretase and γ-secretase cleavage respectively, becoming the infamously toxic $A\beta_{42}$ [4].

The cognitive degradation process links directly to the deficiency in B_6, B_9, and B_{12}, which are vitamins essential to the functioning of the Methionine Cycle [35]. This cycle (enclosed box of Figure 1) encompasses three important physiological functions in normal individuals: regulation of Met and cysteine for protein synthesis, proper DNA and cell growth, and transfer of methyl groups to a broad variety of substrates. The process starts with the introduction of methionine (Met) input (Metin). Methionine is an essential amino acid utilized in protein formation, meaning that it cannot be synthesized by the body, it has to be ingested [33]. As the cycle begins in a normal individual, Met is converted via the enzyme methionine adenosyltransferase (MAT) to S-adenosylmethionine (AdoMet), the most important methyl donor in the body. Next, the donation of a methyl group by AdoMet converts it into S-adenosylhomocysteine (AdoHcy). AdoHcy produces Adenosine and H_2O in a reversible reaction to form Hcy, whose concentration in the brain plays a fundamental role in AD development. Finally, Hcy either undergoes re-methylation to transform back into Met or leaves the cycle as cystathionine, an intermediate in the synthesis of the non-essential amino-acid cysteine. However, this cycle is significantly altered in AD patients, leading to abnormal accumulation of Hcy in the system by reducing the re-methylation rate from Hcy to Met [29]. Research explains that upon the alteration of this cycle, Met oxidizes and binds to $A\beta_{42}$, which increases the protein's toxicity and promotes a more toxic fusion, Met(O)$A\beta_{42}$ [9, 23]. As the toxicity level rises, the brain no longer removes the substance, resulting in polymerization that blocks synaptic activity among neurons [11]. Additionally, studies discovered that AD patients have high levels of Hcy in the brain, which correlates with AD and vascular dementia in elderly affected subjects [28]. While discrepancies exist between whether the oxidation of Met increases or decreases the level of $A\beta_{42}$, for the purpose of our research, we assume Met oxidation will decrease the overall level of $A\beta_{42}$ by means of chemical reactions forming a new compound Met(O)$A\beta_{42}$ (see Figure 3) that will require Met, $A\beta_{42}$ and oxygen [18].

With assistance from the mathematical derivations of the Methionine Cycle [35] and the accumulation of $A\beta_{42}$ [10], this research strives to connect the missing link of two independent systems and create a cycle that occurs in all AD patients. Consequently, we propose a compartmental model with five equations. Particularly, we introduce the compartment, $A\beta_{42}$, to complement Reed's four equations of Met, Hcy, AdoMet, and AdoHcy.

This paper is organized in the following manner: Section B follows from our first assumption, which states a direct connection between the levels of $A\beta_{42}$ and Hcy concentrations. Section C focuses on the relation between Hcy and Met as a function of $A\beta_{42}$ concentration. This relation is portrayed as the principal characteristic dictating the behavior of the disease: increasing concentrations of Hcy and its accumulation in the system. Diagrams, equations, variables and constants related with our model are also described in this section. Section D follows the parameter estimation and discusses the analysis of our simulations. In section E we summarize the results of our studies.

B AD cycle model with an assumed closed loop between $A\beta_{42}$ and Hcy

The following diagram signifies our original proposal with an explicit feedback rate that loops $A\beta_{42}$ back to the Methionine Cycle through Hcy. This case represents a forced biological assumption, where μ_2 is a constant rate that relates $A\beta_{42}$ and Hcy. In this proposal, the term in our equation that represented this relationship was $\pm\ \mu_2 A\beta_{42}$. However, during simulations of this proposal, we noticed no significant changes occurred in the

Methionine Cycle while μ_2 only altered the decay rate of Aβ_{42} level. Thus, we eliminated μ_2 as a parameter and improved this relationship in our model by the introduction of the Aβ_{42} dependant function p (Figure D.1). The following discussion describes the study of μ_2 in the cycle. Although ruled out, this process will gives us insight into determining the right model.

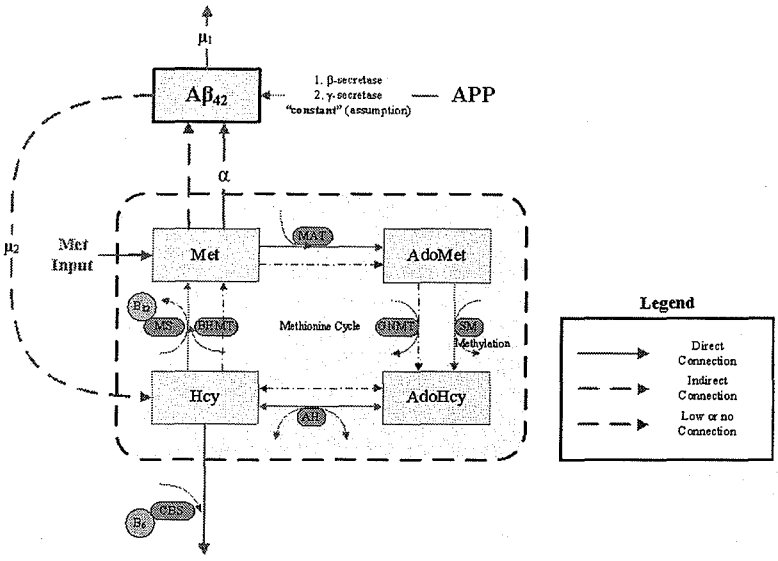

Former Alzheimer's cycle with the trivial assumed closed loop connection between Aβ_{42} and Hcy regulated by the explicit feedback rate μ_2.

The following equations: (93) and (95) were modified (upon the deletion of μ_2) from the original system described in Figure B. This gave rise to our current model equations (98) through (100), Figure C.1, and the necessity of the function p to relate (98) and (100).

$$\frac{d[A\beta_{42}]}{dt} = APP_{A\beta_{42}} - \alpha[Met][A\beta_{42}] - \mu_1[A\beta_{42}] - \mu_2[A\beta_{42}] \tag{93}$$

$$\frac{d[Met]}{dt} = pV_{MS} + pV_{BHMT} + Metin - \alpha[Met][A\beta_{42}] - V_{MATI} - V_{MATIII} \tag{94}$$

$$\frac{d[Hcy]}{dt} = V_{AH} - V_{CBS} - V_{MS} - V_{BHMT} + \mu_2[A\beta_{42}] \tag{95}$$

$$\frac{d[AdoMet]}{dt} = V_{MATI} + V_{MATIII} - V_{GNMT} - V_{METH} \tag{96}$$

$$\frac{d[AdoHcy]}{dt} = V_{GNMT} + V_{METH} - V_{AH}. \tag{97}$$

Upon finding APP$_{A\beta_{42}}$, μ_1, the normal and AD thresholds, we recognized that the magnitude difference of these parameters and that of the other four graphs are approximately 10^5 or 10^6 apart. Therefore, we first converted all of the components in Aβ_{42} by a fitting factor of 5×10^5. We studied the graph of Aβ_{42} independently and observed the behavior as α and μ_2 vary. See Figure B.
With the expected result, we wanted to see how this graph affects the other four compartments in our system, particularly Met and Hcy.

Figures B and B, at α and μ_2 both zero, represent the behavior of normal individuals. Figure B accounts for the fluctuation of varied Metin and 5mTHF while Figure B considers solely fixed constants. Either case serves the purpose of presenting the normal behavior (a control group).

For simplicity, we will only consider Metin and 5mTHF as constants during the rest of our simulations.

In this simulation (Figure B), we set α=0.2 and μ_2=0.2 [1/h]. Simulations for μ_2=0.02, and 0.002 (Figures G.2 and G.2) can be found in the Appendix G.2. While the rate of decay changes in the Aβ_{42} dynamics, no

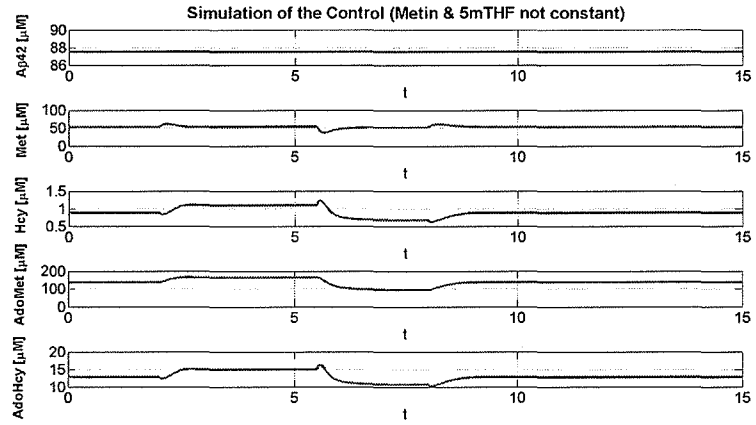

System for healthy individuals (with varied Metin and 5mTHF) α=0 and μ_2=0. The first plot is a general representation of the expected Aβ_{42} behavior. The other four plots are replicated from Reed's model of a normal individual when Metin and 5mTHF are not fixed.

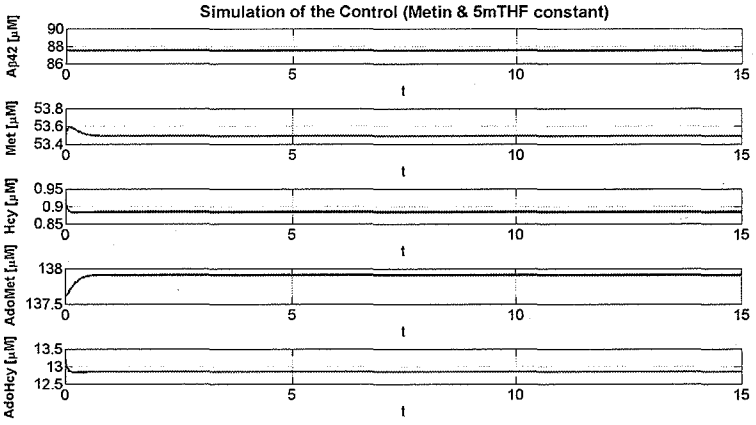

System for healthy individuals (with constant Metin and 5mTHF): Similar to Figure B, the first plot represents a general Aβ_{42} behavior for normal individuals (α=0 and μ_2=0). Although different in appearance, the other four graphs still represent the methionine cycle for normal individuals, but with Metin and 5mTHF as constants.

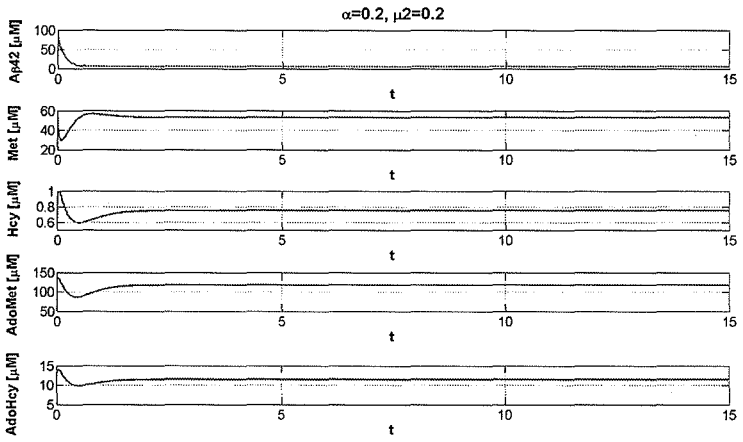

Time series simulations with α=0.2, μ_2=0.2

significant changes occurred in the other four graphs. This contradicts our hypothesis that when α=0.2, Met has substantial connection to Aβ_{42}.

In order to determine the values of μ_2 for which there is a direct effect on the five-compartmental model we simulate the behavior for $\alpha = 1$ and $\mu_2 = 0.002, 0.02$, and 0.2 (Appendix G.2, Figures G.2, G.2, and G.2). We observed, even with a faster decay of Aβ_{42}, the other compartments in our cycle remained the same. With this result, we concluded that μ_2 may not represent the feedback we had expected.

Biologically, this is merely an assumption based on a chain of events. Therefore, we decided to abort the μ_2 connection.

C AD cycle with Aβ_{42} effect in the interaction of Hcy and Met

C.1 Model Descriptions

As APP gets cleaved by β and γ secretases sequentially, we have a production of Aβ_{42} peptide at a rate of $APP_{A\beta_{42}}$ with a natural degradation at rate μ_1 from the body. While the Methionine Cycle regulates the levels of Hcy, some studies suggest that Alzheimer's brains show increased levels of Hcy [29], implying the disruption of the Methionine Cycle, hindering the re-methylation and transsulfuration of Hcy and causing an accumulation within the brain [29]. When this cycle is damaged, the re-methylation from Hcy to Met discontinues, causing a decrease in Met concentrations. Meanwhile, Met residues oxidize into methionine sulfoxide (Met(O)), which binds to Aβ_{42} see Figure C.1. Since compartments, Met and Aβ_{42}, must both contribute in the formation of a new compound [Met(O)Aβ_{42}] at an affinity coefficient of α, Aβ_{42} level is believed to decrease. The mechanism of this reaction follows the laws of mass action. Our hypothesis assumes a connection from the Methionine Cycle to a new compartment, Aβ_{42}, to study AD progression. Our model expands from Reed's model to propose the following Alzheimer's Cycle (Figure C.1).

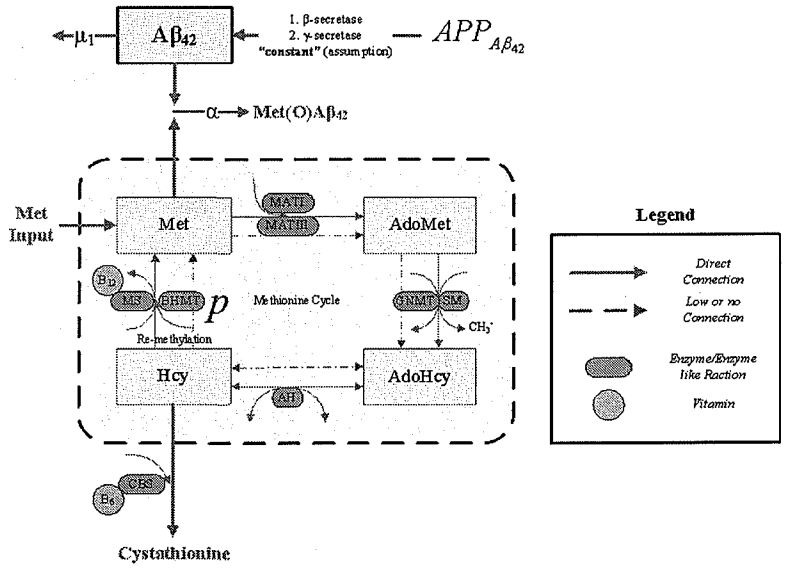

Compartmental model of Alzheimer's Disease cycle. Reed's methionine cycle previously demonstrated the relationship between Hcy, Met, AdoMet, and AdoHcy.

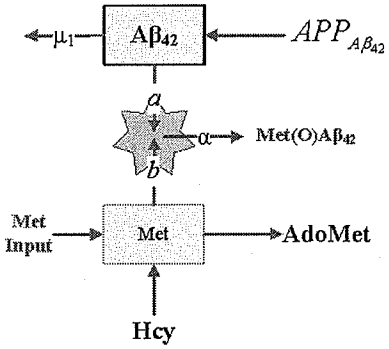

Representation of methionine and Aβ_{42} reaction, previously simplified in our general model (Figure C.1). The rates controlling the individual reactions are "a" for the ongoing reaction of Aβ_{42} binding to methionine sulfoxide, "b" the rate at which methionine oxidizes. These two terms can be described by alpha, an affinity constant that governs the mass action reactions to represent the total output of the new substance α[Met][Aβ_{42}].

C.2 Equation Descriptions

In our model we introduce Aβ_{42} to Reed's 4-dimensional system since there is scientific evidence that Aβ_{42} is relate to Alzheimer's disease. With this addition, we observe the behavior of Reed's equations (particularly Met and Hcy) when the brain's Aβ_{42} concentration level decreases. Tables 1 through 2 give detailed descriptions of all terms (variables and constant values) introduced in the model equations and the properties related with such terms as well as the source of reference. A detailed description of all the terms as found in Reed's paper as well as a table (table (3)) showing specific parameter values, units, values and references for those terms specifically are given in section G.1 located in the Appendix.

$$\frac{d[A\beta_{42}]}{dt} = APP_{A\beta_{42}} - \alpha[Met][A\beta_{42}] - \mu_1[A\beta_{42}] \tag{98}$$

$$\frac{d[Met]}{dt} = pV_{MS} + pV_{BHMT} + Metin - \alpha[Met][A\beta_{42}] - V_{MATI} - V_{MATIII} \tag{99}$$

$$\frac{d[Hcy]}{dt} = V_{AH} - V_{CBS} - pV_{MS} - pV_{BHMT} \tag{100}$$

$$\frac{d[AdoMet]}{dt} = V_{MATI} + V_{MATIII} - V_{GNMT} - V_{METH} \tag{101}$$

$$\frac{d[AdoHcy]}{dt} = V_{GNMT} + V_{METH} - V_{AH}. \tag{102}$$

Equation (98) describes the behavior of Aβ_{42} level. The first term, $APP_{A\beta_{42}}$, is not to be confused as the level of Amyloid Precursor Protein (APP); instead, $APP_{A\beta_{42}}$ represents the level of Aβ_{42} production from APP only. The term, -α[Met][Aβ_{42}] corresponds to equation (98) and describes the outgoing flow of Aβ_{42} once it binds with Met(O) as [Met(O)Aβ_{42}]. It is conveniently described by the laws of mass action as α[Met][Aβ_{42}] where α represents the affinity constant between the Aβ_{42} and Met(O) binding. Furthermore, the term μ_1[Aβ_{42}] is the natural degradation of [Aβ_{42}], where μ_1 is a fixed constant in our study.

Equation (99) models the change in concentration of Met with respect to time. A new term, α[Met][Aβ_{42}], is introduced in addition to Reed's equation. The mechanics of this reaction are the same as the ones described in the previous paragraph. This is due to the fact that the outflow of α[Met][Aβ_{42}] (negative sign) is the same for both substances (mass action). Figure C.1 depicts the specifics of this reaction. It is important to note that the term "Metin" is described by Reed as metionine input; while he gave several value this term, we will give it a fixed value of 200 μM.

Equation (100) models the change in levels of homocysteine with respect to time. Equation 100, is slightly altered from the original expression in Reed's model since we are taking into account a new element in the cycle, Aβ_{42}. The p (Figure D.1) in both equation (99) and (100) is a function of Aβ_{42}. In essence, when Aβ_{42} level is at 87.5μM (1.75×10^{-4} times the scaling factor 5×10^5) to account for the magnitude difference between these quantities, the condition for normal individuals [18], p equals 1; this implies that the connection between Hcy and Met is successfully operating. However, when Aβ_{42} level decreases to the AD threshold, 43.35 μM (8.67×10^{-5} times 5×10^5), p approaches 0 and the re-methylation of Hcy is no longer effective. Between these two conditions, p is modeled by a function dependent on concentrations of Aβ_{42} (See equation 103). We used a conversion factor (5×10^5) to have comparable magnitudes in our calculations. Since the magnitudes for Reed's model metabolites (Hcy, Met, AdoMet and AdoHcy) range between 1 and 300, and since the main goal of our investigation is to portray the qualitative aspects of AD development, it helps, for comparison purposes, to have the Aβ_{42} concentration in similar magnitude values.

Finally, equations (101) and (102) are exact replicates of Reed's model of AdoMet and AdoHcy respectively. While these equations remain identical, the behaviors may alter significantly since all of the equations in the system are interrelated. Metabolites Hcy, Met, and peptide Aβ_{42} will be analyzed in depth due to its connection to AD resources and linkage with the neurological disease.

Variable	Units	Description
$[Met]$	μM	Methionine concentration
$[A\beta_{42}]$	μM	Amyloid-β 42 concentration
$[Hcy]$	μM	Homocysteine concentration
$[AdoMet]$	μM	S-adenosylmethionine concentration
$[AdoHcy]$	μM	S-adenosylhomocysteine concentration

Table 1: Time-dependent Variables

As stated before, the expressions in equations (99) through (102) displayed as V's with different subscripts are found in section G.1 located in the Appendix; these expressions show a high non-linear behavior, and show every single constant and variable term on them. With the current descriptions of equations (99) through (102) and their related terms, it becomes difficult to appreciate the interactions that the variables show in the system. To facilitate and further understand the dynamics of our model we can simplify the V's defined by Reed into simpler functions in terms of variables by substituting all the parameter values in the V's. We call this functions F; for example, F_1=V_{MS}, F_2=V_{BHMT}, etc.

Then, our differential equations system is defines as:

$$\begin{aligned}
\frac{d[A\beta_{42}]}{dt} &= APP - \alpha[A\beta_{42}][Met] - \mu_1[A\beta_{42}] \\
\frac{d[Met]}{dt} &= p(F_1 + F_2) + Metin - \alpha[A\beta_{42}][Met] - F_3 - F_4 \\
\frac{d[Hcy]}{dt} &= F_7 - F_8 - p(F_1 + F_2) \\
\frac{d[AdoMet]}{dt} &= F_3 + F_4 - F_5 - F_6 \\
\frac{d[AdoHcy]}{dt} &= F_5 + F_6 - F_7
\end{aligned}$$

where

$$\begin{aligned}
F_1 &= \frac{1.3 \times 10^5[Hcy]}{31 + 1510[Hcy]}, \\
F_2 &= \frac{62.5(178 - [AdoMet] - [AdoHcy])[Hcy]}{12 + [Hcy]}, \\
F_3 &= \frac{561[Met]}{[Met] + 0.82[AdoMet] + 41}, \\
F_4 &= \frac{2.287 \times 10^4[Met]([Met] + 21.1)(1 + 5.7(\frac{[AdoMet]}{[AdoMet]+600})^2)}{[Met]([Met] + 21.1)(1 + 5.7(\frac{[AdoMet]}{[AdoMet]+600})^2) + 4.22 \times 10^5}, \\
F_5 &= \frac{1.06 \times 10^4[AdoMet]^{2.3}}{([AdoMet]^{2.3} + 2.5257 \times 10^8)(1 + \frac{1}{20}[AdoHcy])}, \\
F_6 &= \frac{411[AdoMet]}{[AdoMet] + (1 + \frac{1}{4}[AdoHcy])}, \\
F_7 &= 100([AdoHcy] - 10[Hcy]), \\
F_8 &= (1.7[AdoMet] + 1.7[AdoHcy] - 30)[Hcy].
\end{aligned}$$

We can now observe the role that the variables described in table 1 play in our system. We are now ready to analyze the different aspects of a normal person and an AD patient by using our model with the right parameters and the aid of computer simulations.

D Analysis

D.1 Parameter Estimation

The term $\text{APP}_{A\beta_{42}}$, as previously described, is the $A\beta_{42}$ production level. Research suggests this parameter maintains constant regardless of AD's severity. As a result, we found out this parameter from the initial condition and $A\beta_{42}$'s natural degradation rate [18, 34].

The constant value α is the most complicated parameter in our system since it is the rate at which Met oxidizes and binds with $A\beta_{42}$ (refer to Figure C.1 for details). Table 3 shows the parameters used throughout this investigation.

Parameters	Description	Units	Value	References
$APP_{A\beta_{42}}$	$A\beta_{42}$ cleavage from APP[§]	$\mu M/time$	66.75	[18],[34]
μ_1	degradation rate of $A\beta_{42}$	time^{-1}	0.763	[34]
α	methionine sulfoxide $A\beta_{42}$ mass action constant	$1/(\mu M \cdot time)$	0.2	fitted

Table 2: Parameters for the Proposed Alzheimer's Disease Model
[§]Amyloid Precursor Protein

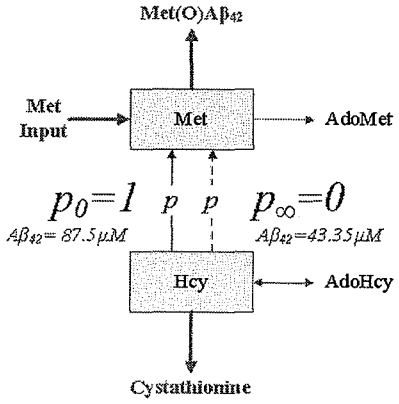

Function p defined as a function of $A\beta_{42}$ concentration and its relationship with the Alzheimer's cycle

We claim that the amount of Hcy converted to Met depends on the concentration of $A\beta_{42}$ in the brain, since it is known that the concentration of Hcy is related to the severity of AD, which in turn depends on the amount of $A\beta_{42}$ in the brain [18]. We can assume that there is a function p that can be described as an implicit feedback into the Methionine Cycle (Figure D.1). While this function is not explicitly shown as the feedback in our diagram (Figure C.1), it will actually depend on the level of $A\beta_{42}$. In other words, when $A\beta_{42}$ level decreases from initial condition to AD threshold, p, is defined as follows:

$$p_k([A\beta_{42}]) = \frac{\frac{APP_{A\beta_{42}}}{\mu_1}}{\frac{APP_{A\beta_{42}}}{\mu_1} + k\left(\frac{APP_{A\beta_{42}}}{\mu_1} - [A\beta_{42}]\right)}. \tag{103}$$

The expression $\frac{APP_{A\beta_{42}}}{\mu_1}$ comes from the fact that a normal person has a constant change of $A\beta_{42}$ concentration, thus its variable will equal to zero. Also, biologically for a normal methionine cycle, the oxidation of methionine will be insignificant. This is the same as saying α=0. This can be verified in equation (98). After

the corresponding substitutions and rearrangements in equation (98), we end up with $[A\beta_{42}]=\frac{APP_{A\beta_{42}}}{\mu_1}$. Then, we can state that:

$$p_k([A\beta_{42}]) = \frac{\varphi}{\varphi + k\,(\varphi - [A\beta_{42}])} \tag{104}$$

where

$\varphi = \frac{APP_{A\beta_{42}}}{\mu_1}$ (level of $A\beta_{42}$ concentration in a normal person).

The introduction of function p represents the chain of events that lead to AD according to our biological assumptions. Damaged neurons from Met(O)$A\beta_{42}$ polymerization cause AD; in addition, studies discovered that most types of dementia, especially AD, is related with a deficiency of vitamins B_6, B_9, and B_{12}, which are essential to the re-methylation of Hcy to Met (governed by function p). With this methylation process, Hcy compiles and Met is no longer recycled. In conclusion, a decrease in the level of $A\beta_{42}$ leads to a discontinuity of Hcy-to-Met connection, which increases Hcy level and decreases Met level [23, 29].

We have considered the direct connection between Hcy and Met as a function of $A\beta_{42}$, such that p is bounded between 0 and 1. We set $p = 1$ for a normal person, where the $A\beta_{42}$ threshold is approximately 87.5 μM, indicating a stable connection between Hcy and Met. With a decrease of $A\beta_{42}$ below this threshold, we assume the pre-clinical stages of AD have occurred. When the level reaches a concentration around 43.4 μM, the threshold for clinical diagnosed AD, individuals are considered to be Alzheimer's patients. At this point, p is really small, suggesting no connection between the compartments and causing no clogging of Hcy in the brain. Oxidation of Met residues, which cause increase of $A\beta_{42}$ toxicity by binding with it (refer to Figure C.1), will be minor for minor values of p.

$$p_0(\varphi) = 1 \tag{105}$$

and

$$p_k\left(\frac{APP_{A\beta_{42}}}{2\mu_1}\right) \longrightarrow 0 \quad \text{for } k \text{ big enough.} \tag{106}$$

For expression (104) we define the following conditions:

- For a normal person the threshold of $A\beta_{42}$ concentration is:
  $[A\beta_{42}] = \frac{APP_{A\beta_{42}}}{\mu_1} = \varphi = 87.5\mu M$ (from the initial condition of $A\beta_{42}$ in (1)).
- The second threshold occurs at:
  $[A\beta_{42}] = \frac{APP_{A\beta_{42}}}{2\mu_1} = \varphi/2 = 43.35\mu M$

  where $\varphi/2$ is the threshold concentration of $A\beta_{42}$ when AD starts to significantly impair cognitive abilities of a person.

The region between the thresholds represents the onset of AD and is depicted in Figure D.1.
We finally get equation which represents the values that p will take as $A\beta_{42}$ changes:

$$p_k(A\beta_{42}) = \frac{87.5}{87.5 + k\,(87.5 - [A\beta_{42}])}. \tag{107}$$

D.2 Simulations

For this model we introduced the implicit feedback p (Figure D.1). With no previous studies on our parameter α, we must first find a logical approximation before we gain more meaningful simulations. To find α, we fixed all known values, varied α in a large range of reasonable numbers, and executed several simulations in loops (Figure D.2).

In previous simulations, we noticed that $A\beta_{42}$ reaches a steady state in the time interval from 10 to 20. Consequently, we created a scatter plot of the steady states for $A\beta_{42}$ as α varies. From the graph (Figure D.2), there appears a rapid decrease when α is between 0 and 0.1, which suggests that α is too small and the decay

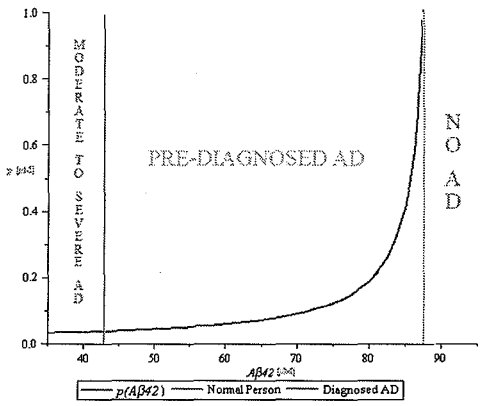

Plot of p with respect of $A\beta_{42}$ with different levels of AD severity.

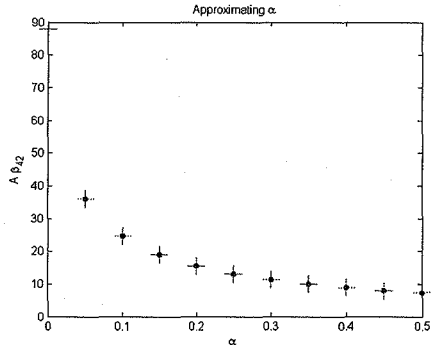

The parameter α is selected at 0.2, where the graph of α vs. $A\beta_{42}$ begins to approach a steady state.

in $A\beta_{42}$ may reach steady state prior to the AD threshold. Furthermore, when α reaches 0.4, the steady states of $A\beta_{42}$ is approaching a horizontal line, which suggests the decay occurs too rapidly and $A\beta_{42}$ level reaches steady state immediately and remains there. Figure D.2a and D.2b each represent the extremes we omitted, granting us a range of α to select.

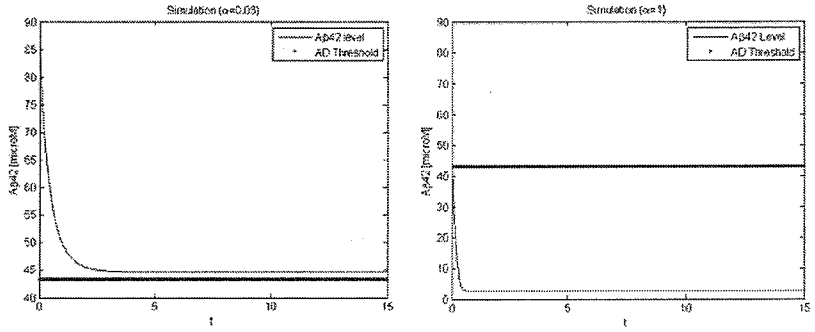

(a) $A\beta_{42}$ Simulation for a small α (α=0.03): The decay never reaches the AD threshold, implying a value is too small to give a correct representation of our model. (b) $A\beta_{42}$ Simulation for big α (α=1): The decay immediately reaches the AD threshold, implying a value is too big to give a feasible representation of our model.

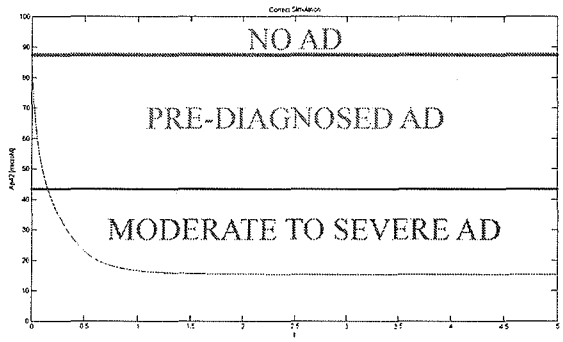

Qualitative Stages of AD: The thicker horizontal line at 87.5 represents the threshold of a healthy individual and the thinner horizontal line at 43.35 represents the threshold for Alzheimer's. As $A\beta_{42}$ level decreases in an AD patient, the individual, according to the graph, will experience all the stages listed.

Upon careful consideration, we selected a reasonable value for α in between 0.0 and 0.2 to represent an ideal AD behavior. In the above simulations as α=0.2 (Figure D.2), we observe the behavior of a typical AD patient. A healthy individual's $A\beta_{42}$ level should have an overall steady state at the horizontal line at 87.5 $[\mu M]$ (control threshold). The horizontal line at 43.35 $[\mu M]$ is the AD threshold, indicating a clinical diagnosis. The decay of $A\beta_{42}$ reaches all three regions of the graph, showing the early, mild, and severe stages of AD. This is also shown in the derivation of p_k in equations (103) through (107)and Figure D.1.

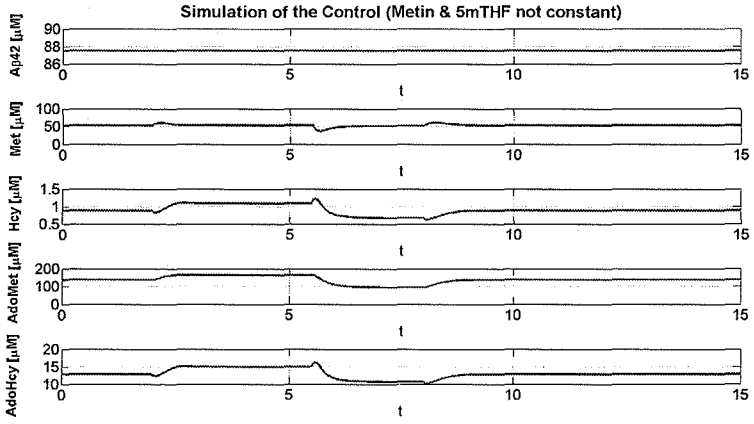

Simulations of system with ideal parameters (varied Metin and 5mTHF).

After a study of the dynamics of $A\beta_{42}$ in isolation, we now unite the 5 compartments to observe the interrelated connection that may take place. For comparison purposes, Figure D.2 treats Metin and 5mTHF as functions and illustrates the fluctuation of all 5 compartments. Particularly, we noticed the expected decay of the levels of concentration of $A\beta_{42}$ and Met, and a fast increase on the levels of Hcy. Thus there appears a slight increment of the $A\beta_{42}$ levels during the time interval from 5 to 10, in which Met and Hcy levels decay before reaching steady states. More importantly, the overall behaviors of our three compartments of focus confirmed our prediction: Hcy level increases, Met level decreases, and $A\beta_{42}$ level decreases. When Metin and 5mTHF are not constants, there appear fluctuations, demonstrating how each compartment absorbs the alterations of supply (Metin, 5mTHF). However, the overall behavior in the long run appears to be accurate, which is our focus. Since the fluctuation may cause some uncertainty, we set Metin and 5mTHF as constants in Figure D.2 to eliminate doubt.

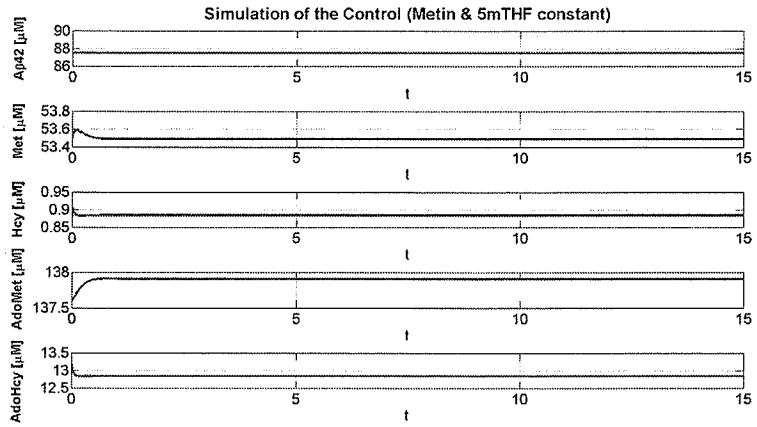

Simulations of system with ideal parameters (constant Metin and 5mTHF): Unlike Figure D.2, this eliminates the fluctuation, simplifying the analysis of the general behavior.

With Metin and 5mTHF as constants, there are no confusing fluctuations; instead there appears only a smooth curve. As Hcy increases, Met decreases, which is biologically supported in AD patients. When individuals lack vitamins, the connection between Hcy and Met is no longer supportable, resulting in an accumulation of Hcy and a stoppage in the recycling of Met. Furthermore, there is a smooth decay of the Aβ_{42} concentrations, which biologically is predicted as well. When the recycled Met is no longer feasible, an oxidation process occurs, allowing the binding of more toxic product Met(O)Aβ_{42}. In this process, both Met and Aβ_{42} must contribute, resulting in decays in the graphs of both concentrations.

We put our attention on the first three plots in Figure D.2, the main metabolites (Aβ_{42}, Met and Hcy) analyzed in AD. For a better comparison between these metabolites, we plotted three other graphs (Figures D.2a, D.2b and D.2c), each of which compares two metabolites in the same plot.

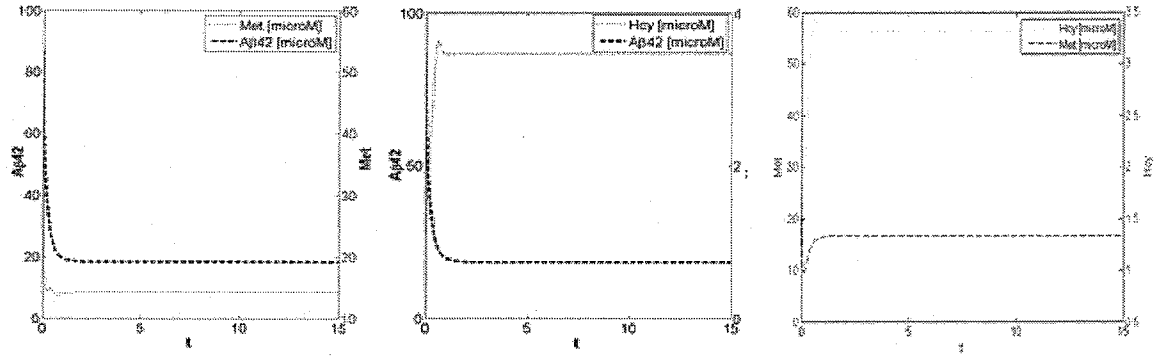

(a)Comparison between Aβ_{42} and Met: with Aβ_{42} overlapping Met in the same frame, the effects of one on the other is easily observed.(b)Comparison between Aβ_{42} and Hcy: with Aβ_{42} overlapping Hcy in the same frame, the contrasts of both graphs are made visible.(c)Comparison between Met and Hcy: with Met overlapping Hcy in the same frame, the direct behavior of the two compartments are further explored.

A comparison between Aβ_{42} and Met is illustrated in Figure D.2(a). In this graph, both Aβ_{42} and Met show similar decay rate and reaches steady state simultaneously, which is further evidence for the biological dynamics of AD discussed in this paper.

We compare Aβ_{42} and Hcy in Figure D.2(b). While both compartments reach a steady state simultaneously, there is clear dissimilarity between the behaviors, where Aβ_{42} decreases as Hcy increases. Again, this is the biological prediction, which validates our model accurately monitors the behavior of AD.

Met and Hcy are depicted in Figure D.2(c). The decrease, increase, and detailed fluctuations are reflected. As Hcy increases due to its inability to recycle Met, Met decreases at the exact same proportion. All three graphs demonstrated agreements between the biological observation and our mathematical model.

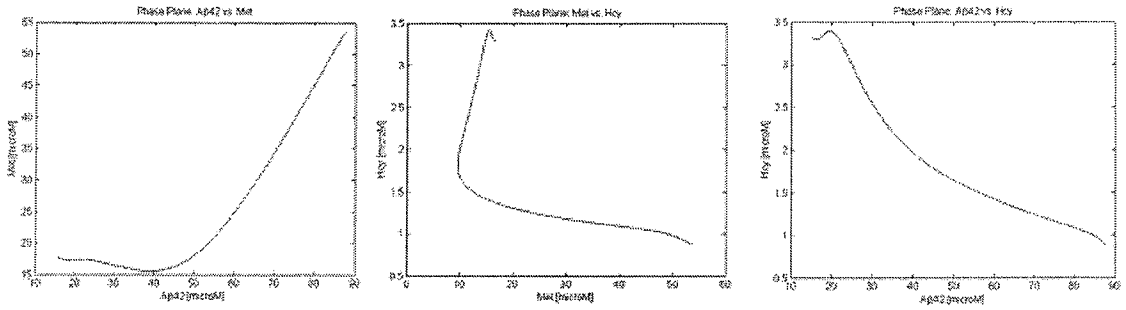

(a) Phase plane showing the concentrations of Met vs. Aβ_{42} in Alzheimer's Disease, (b)Phase plane showing the concentrations of Met vs. Hcy in Alzheimer's Disease (c) Phase plane showing the concentrations of Aβ_{42} vs. Hcy in Alzheimer's Disease.

To further explore the relationship among these three compartments (Aβ_{42}, Met, Hcy) we simulated the phase plane to see the behavior of one compartment as the result of another. A phase plane is represented in Figure D.2(a), which provides a relationship between Aβ_{42} and Met. First, the phase plane graph starts at initial condition (Aβ_{42},Met)=(87.5,53.5), and gives an almost linear decrease until approximately (42;15) μM where the first entry represents the concentration of Aβ_{42} and the second the concentration of Met in the phase plane. This behavior agrees with the one shown in the methionine-Alzheimer's Disease cycle for a person with AD: decreasing levels of Aβ_{42} caused by its binding with Met (as depicted in Figure 3 Aβ_{42} actually binds to Met(O)Aβ_{42} under the laws of mass action at a constant rate α) also showed a decrease of Met [18, 29]. For lower levels of Aβ_{42} (42 to 15), Met behaves unexpectedly; it actually increases. This, however, represents an insignificant increase (about two units from 15 to 17) which represents only $2/38 \approx 0.053$ μM of the total change that Met underwent at the beginning. At (15;17) a steady state is finally reached.

The relationship between Met and Hcy concentrations in an AD patient is shown in Figure D.2(b). This phase plane shows how the concentrations of Met, decreases from an initial value of about 54 μM to about 25 μM. This change is accompanied by an increment in the concentration of Hcy. Hcy increases from about 0.8 to about 3.4 μM. However, it is important to note that the change from (54;7) to (11;1.5) μM is the one predicted biologically. The behavior from (11;1.5) to (17;3.25) μM is insignificant in terms of Met concentration change. Hcy, however, continued to rise. This fluctuation is present due to the complexity of the methionine cycle and the interactions between all the four metabolites at all times. Again, a steady state is finally reached for Hcy and Met concentrations.

The phase plane represented in Figure D.2(c) depicts the behavior between the concentration of Aβ_{42} and Hcy in an AD patient. Disregarding the scale used, the decrease of Aβ_{42} is also accompanied by an almost uniform decrease in Hcy concentration. By this we mean that the scale used did not influenced the effects we predicted from the theory. Since the function p which dictates the concentration of Hcy in the system, depends on the concentration of Aβ_{42}, Hcy increases for low levels of Aβ_{42}. Again, little insignificant fluctuations are present at the upper leftmost part of the figure before reaching a steady state.

E Conclusion

Currently, there is a big concern about the increase incidences of Alzheimer's disease among the elderly population. As the seventh leading cause of death in the United States, scientists are struggling to cure this devastating disease. While there is no knowledge of the exact cause, there are various theories. Among these

hypotheses on the cause of the disease, we directed our attention towards the concentrations of $A\beta_{42}$ in AD patients' brains.

In this work, we built on Reed's methionine cycle by introducing our compartment of focus, $A\beta_{42}$, in order to study the qualitative behaviors of AD's initiation and progression. Particularly, we designed a five-compartment mathematical model to represent the relationship among the concentrations of specifically $A\beta_{42}$, Hcy, and Met. We performed simulations to see the relationships between $A\beta_{42}$ and the methionine cycle compartments. Since previous studies show that AD patients suffer from high levels of Hcy in their brain [29], we made a biological assumption to suggest a direct connection between $A\beta_{42}$ and Hcy compartments (Figure C.1). With this as our first proposal, behaviors of the compartments were simulated. As the values for α and μ_2 vary, only the $A\beta_{42}$ concentration appeared to decay while there were no significant changes in the behavior of the methionine cycle, opposing our biological findings. Thus we decided to modify our model by eliminating the explicitly direct connection from $A\beta_{42}$ to Hcy.

Through different methods, we were able to estimate all the parameters prior meaningful simulations. Upon finding correct parameters, simulations showed the expected behavior corresponding to biological support–AD patients have a decrease in $A\beta_{42}$ level, a decrease in Met level, and an increase in Hcy [18, 29].

Since none of our research on AD showed that previous studies took into account the interaction between the methionine cycle and the concentrations of $A\beta_{42}$, our model is based on biologically assumptions. Quantitative properties of AD, such as time units and concentration thresholds for all of our compartments are based on this qualitative consideration. However, our model qualitatively replicates the biological discoveries with numerical simulations. Additionally, all of our assumed connections granted biologically predicted behaviors of the compartments in our cycle. When accurate data is applied to our model's qualitative results, parameters may easily be varied to study the exact phenomenon of AD. If our assumptions are accurate, researchers may use data to model the disease under certain parameters to retrieve significant information. Even if data is not present, future researchers may apply optimal control theory to compare treatments' qualitative effects on delaying the disease. In fact, when the initiation of AD is observed numerically, there are many possibilities to delay or even prevent the progression.

F Acknowledgment

The MTBI/SUMS Summer Undergraduate Research Program is supported by The National Science Foundation (DMS-0502349); The National Security Agency (DOD-H982300710096); The Sloan Foundation; Research Initiative for Student Enhancement (RISE GM59429); and Arizona State University. Particularly, our research topic owes a special appreciation to Dr. Carlos Castillo-Chávez for granting this opportunity. Additionally, the success of the project is a result of the wonderful assistance from Dr. Abdessamad Tridane, Dr. Joaquín Rivera, David Tello, and Griselle Torres-García.

References

[1] Alzheimer's Association. (2008). Stages of alzheimer's. Retrieved July 10, 2008, from http://www.alz.org/alzheimers_disease_stages_of_alzheimers.asp

[2] Banerjee, R., Chen, Z., & Gulati, S. (1997). Methionine synthase from pig liver. Methods in Enzymology, 281, 189-197.

[3] Banerjee, R. V., Frasca, V., Ballou, D. P., & Matthews, R. G. (1990). Participation of cob(I)alamin in the reaction catalyzed by methionine synthase from escherichia coli: A steady-state and rapid reaction kinetic analysis. Biochemistry, 29(50), 11101-11109.

[4] Bitan, G., Kirkitadze, M. D., Lomakin, A., Vollers, S. S., Benedek, G. B., & Teplow, D. B. (2003). Amyloid β-protein (Aβ) assembly: Aβ40 and Aβ42 oligomerize through distinct pathways. Proceedings of the National Academy of Sciences of the United States of America, 100(1), 330-335.

[5] Borcsok, E., & Abeles, R. (1982). Mechanism of action of cystathionine synthase. Archives of Biochemistry and Biophyics., 213, 695-707.

[6] Brown, F. C., & Gordon, P. H. (1971). Cystathionine synthase from rat liver: Partial purification and properties. Canadian Journal of Biochemistry, 49(5), 484-491.

[7] Cabrero, C., Puerta, J., & Alemany, S. (1987). Purification and comparison of two different forms of S-adenosyl-L-methionine synthase from rat liver. European Journal of Biochemistry, 170, 299-304.

[8] Cabrero, C., & Alemany, S. (1988). Conversion of rat liver S-adenosyl-L-methionine synthetase from high-mr form to low-mr form by LiBr. Biochimica Et Biophysica Acta, 952(3), 277-281.

[9] Ciccotosto, G., Barnham, K., Cherny, R., Masters, C., Bush, A., Curtain, C., et al. (2003). Methionine oxidation: Implications for the mechanism of toxicity of the β-amyloid peptide from alzheimer's disease. Letters in Peptide Science, 10(1), 413-417.

[10] Craft, D. L., Wein, L. M., & Selkoe, D. J. (2002). A mathematical model of the impact of novel treatments on the Aβ burden in the Alzheimers brain, CSF and plasma. Bulletin of Mathematical Biology, 64(5), 1011-1031.

[11] De la Vega, R., & Zambrano, A. (2008). La circunvalacin del hipocampo. Retrieved July 10, 2008, from http://www.hipocampo.org/alzheimer.asp

[12] Selkoe, D. J. (2001). Alzheimer's disease: Genes, proteins, and Therapy. Physiological Reviews, 81, 741-766.

[13] Duerre, J. A., Wallwork, J. C., Quick, D. P., & Ford, K. M. (1977). In vitro studies on the methylation of histones in rat brain nuclei. The Journal of Biological Chemistry, 252(17), 6981-6985.

[14] Finkelstein, J. D., Harris, B. J., & Kyle, W. E. (1972). Methionine metabolism in mammals: Kinetic study of betaine-homocysteine methyltransferase. Archives of Biochemistry and Biophysics, 153(1), 320-324.

[15] Finkelstein, J. D., & Martin, J. J. (1984). Methionine metabolism in mammals. distribution of homocysteine between competing pathways. The Journal of Biological Chemistry, 259(15), 9508-9513.

[16] Finkelstein, J. D., & Martin, J. J. (1986). Methionine metabolism in mammals. adaptation to methionine excess. The Journal of Biological Chemistry, 261(4), 1582-1587.

[17] Finkelstein, J. D. (1990). Methionine metabolism in mammals. The Journal of Nutritional Biochemistry, 1(5), 228-237.

[18] Gloeckner, S. F., Meyne, F., Wagner, F., Heinemann, U., Krasnianski, A., Meissner, B., et al. (2008). Quantitative analysis of transthyretin, tau and amyloid-beta in patients with dementia. Journal of Alzheimer's Disease : JAD, 14(1), 17-25.

[19] Hoffman, J., & Cornatzer, W. (1978). Fractionation of methionine adonosyltransferase isozymes (rat liver). Methods of enzymology 94, 223-228.

[20] Hoffman, D. R., Cornatzer, W. E., & Duerre, J. A. (1979). Relationship between tissue levels of S-adenosylmethionine, S-adenylhomocysteine, and transmethylation reactions. Canadian Journal of Biochemistry, 57(1), 56-65.

[21] Hoffman, J. L. (1983). Fractionation of methionine adenosyltransferase isozymes (rat liver). Methods in Enzymology, 94, 223-228.

[22] Kandel, E. R., Schwartz, J. H., & Jessell, T. M. (2000). Principles of Neural Science (4th ed.). New York; London: McGraw-Hill Health Professions Division.

[23] Hou, L., Kang, I., Marchant, R. E., & Zagorski, M. G. (2002). Methionine 35 oxidation reduces fibril assembly of the amyloid abeta-(1-42) peptide of alzheimer's disease. The Journal of Biological Chemistry, 277(43), 40173-40176.

[24] Kashiwamata, S., & Greenberg, D. M. (1970). Studies on cystathionine synthase of rat liver. properties of the highly purified enzyme. Biochimica Et Biophysica Acta, 212(3), 488-500.

[25] Kerr, S., & Headly, J. (1974). Modulation of tRNA methyltransferase activity by competing enzyme systems. Advances in Enzyme Regulation, 12, 4248-4252.

[26] Kumar, V., & Eisdorfer, C. (1998). Advances in the diagnosis and treatment of alzheimer's disease. New York: Springer Pub. Co

[27] Martinov, M. V., Vitvitsky, V. M., Mosharov, E. V., Banerjee, R., & Ataullakhanov, F. I. (2000). A substrate switch: A new mode of regulation in the methionine metabolic pathway. Journal of Theoretical Biology, 204(4), 521-532.

[28] McCaddon, A. M., Regland, B. MD, PhD, Hudson, P. M., & Davies, G. M. (2002). Functional vitamin B-12 deficiency and alzheimer disease. Medical Hypothesis, 58(9)(1), 1395-1399.

[29] Miller, A. R. (2003). The methionine-homocysteine cycle and its effects on cognitive diseases - homocysteine & cognitive. Retrieved July 15, 2008, from http://findarticles.com/p/articles/mi_m0FDN/is_1_8/ai_98540119

[30] Nakagawa, H., & Kimura, H. (1968). Purification and properties of cystathionine synthetase synthetase from rat liver: Separation of cystathionine synthetase from serine dehydratase. Biochemical and Biophysical Research Communications, 32(2), 209-214.

[31] National Center for Health Statistics. (2008). Alzheimer's disease. Retrieved July 10, 2008, from http://www.cdc.gov/nchs/fastats/alzheimr.htm

[32] Ogawa, H., & Fujioka, M. (1982). Purification and properties of glycine N-methyltransferase from rat liver. Journal of Biological Chemistry, 257, 3447-3452.

[33] Otten, J. J., Hellwig, J. P., & Meyers, L. D. (2006). DRI, dietary reference intakes :The essential guide to nutrient requirements. Washington, D.C.: National Academies Press.

[34] Perez, A., Morelli, L., Cresto, J. C., & Castano, E. M. (2000). Degradation of soluble amyloid beta-peptides 1-40, 1-42, and the dutch variant 1-40Q by insulin degrading enzyme from alzheimer disease and control brains. Neurochemical Research, 25(2), 247-255.

[35] Reed, M. C., Nijhout, H. F., Sparks, R., & Ulrich, C. M. (2004). A mathematical model of the methionine cycle. Journal of Theoretical Biology, 226(1), 33-43.

[36] Sullivan, D. M., & Hoffman, J. L. (1983). Fractionation and kinetic properties of rat liver and kidney methionine adenosyltransferase isozymes. Biochemistry, 22(7), 1636-1641.

[37] Trysberg, E., Hglund, K., Svenungsson, E., Blennow, K. & Tarkowski, A. (2004). Decreased levels of soluble amyloid B-protein precursor and B-amyloid protein in cerebrospinal fluid of patients with systemic lupus erythematosus. Retrieved July 15, 2008, from http://www.medscape.com.ezproxy1.lib.asu.edu/viewarticle/468489

[38] Yeo, E. J., & Wagner, C. (1992). Purification and properties of pancreatic glycine N-methyltransferase. The Journal of Biological Chemistry, 267(34), 24669-24674.

G APPENDIX

G.1 Detailed expressions from Reed's model in equations (98) to (102)

Enzyme	Parameter	Units	Value	References
$MATI$	V_{max}^{MATI}	$\mu M/h$	561	[27],[8],[21]
	K_m^{MATI}	μM	41	[27],[36]
	K_i^{MATI}	μM	50	[27],[8],[36],[7]
$MATIII$	V_{max}^{MATIII}	$\mu M/h$	22,870	[27],[8],[21]
	K_{m1}^{MATIII}	μM	†	[27],[36]
	K_{m2}^{MATIII}	μM	21.1	[27],[36]
$GNMT$	V_{max}^{GNMT}	$\mu M/h$	10,600	[27],[32],[38]
	K_m^{GNMT}	μM	4500	[27],[32]
	K_i^{GNMT}	μM	20	[27],[25]
$Methylation$	V_{max}^{METH}	$\mu M/h$	4521	[27]
	K_{m1}^{METH}	μM	†	[27],[13],[19]
	$\frac{K_{m2}^{MATIII}}{[A]}$	–	10	[35],[27],[13],[19]
AH	V_{AH}	$\mu M/h$	†	[35],[20]
	α_1	1/h	100	[35]
	α_2	None	10	[35]
CBS	V_{CBS}	$\mu M/h$	†	[35],[15],[16],[30],[24],[6],[5]
	β_1	$1/\mu M$ h	1.7	[35]
	β_2	$(h)^{-1}$	30	[35]
MS	V_{max}^{MS}	$\mu M/h$	500	[35],[16],[2]
	$K_{m,Hcy}^{MS}$	μM	0.1	[2]
	$K_{m,5mTHF}^{MS}$	μM	25	[2]
	K_d^{MS}	μM	1	[3]
$BHMT$	V_{max}^{BHMT}	$\mu M/h$	2500	[35],[15],[17]
	K_m^{BHMT}	μM	12	[35],[14]

† depends on variables.

Table 3: Rate Constants and References

It is necessary to indicate that since our study is dedicated towards a qualitative perspective, the values given here are multiplied by a factor of 5×10^5 during simulations to account for the difference between the concentration magnitudes of Aβ_{42} and those in Reed's study.

$$V_{MATI} = \frac{V_{max}^{MATI}}{1+\frac{K_m^{MAT}}{[Met]}\left(1+\frac{[AdoMet]}{K_i^{MATI}}\right)} \tag{108}$$

$$V_{MATIII} = \frac{V_{max}^{MATIII}}{1+\frac{K_{m1}^{MATIII}K_{m2}^{MATIII}}{[Met]^2+[Met]K_{m2}^{MATIII}}} \tag{109}$$

where

$$K_{m1}^{MATIII} = \frac{20000}{1 + 5.7\left(\frac{[AdoMet]}{[AdoMet]+600}\right)^2} \tag{110}$$

Also

$$V_{GNMT} = \frac{V_{max}^{GNMT}}{1 + \left(\frac{K_m^{GNMT}}{[AdoMet]}\right)^{2.3}} \frac{1}{1 + \frac{[AdoHcy]}{K_i^{GNMT}}} \tag{111}$$

$$V_{METH} = \frac{V_{max}^{METH}}{1 + \frac{K_{m1}^{METH}}{[AdoMet]} + \frac{K_{m2}^{METH}}{[A]} + \frac{K_{m2}^{METH}}{[A]} \frac{K_{m1}^{METH}}{[AdoMet]}} \tag{112}$$

$$K_{m1}^{METH} = 1.0\left(1 + \frac{[AdoHcy]}{4}\right) \tag{113}$$

$$\frac{K_{m2}^{METH}}{[A]} = 10 \tag{114}$$

$$V_{MS} = \frac{V_{max}^{MS}[5mTHF][Hcy]}{K_d^{MS}K_{m,Hcy}^{MS} + K_{m,Hcy}^{MS}[5mTHF] + K_{m,5mTHF}^{MS}[Hcy] + [5mTHF][Hcy]} \tag{115}$$

$$V_{AH} = \alpha_1\left([AdoHcy] - \alpha_2[Hcy]\right) \tag{116}$$

$$V_{CBS} = \left(\beta_1\left([AdoMet] + [AdoHcy]\right) - \beta_2\right)[Hcy] \tag{117}$$

$$V_{BHMT} = (0.7 - (0.025)([AdoMet] + [AdoHcy] - 150))\frac{V_{BHMT}^{max}[Hcy]}{K_m^{BHMT} + [Hcy]} \tag{118}$$

$5mTHF$ is a substrate for the conversion of Hcy and Met. It was selected between certain ranges by Reed (5.2 to 7.2 μM) for a certain amount of time to observe the behavior of the methionine cycle. In our stydy, 5mTHF is fixed at $5.2\mu M/\text{h}$.

G.2 Simulations showing minimal connection between μ_2 and the system

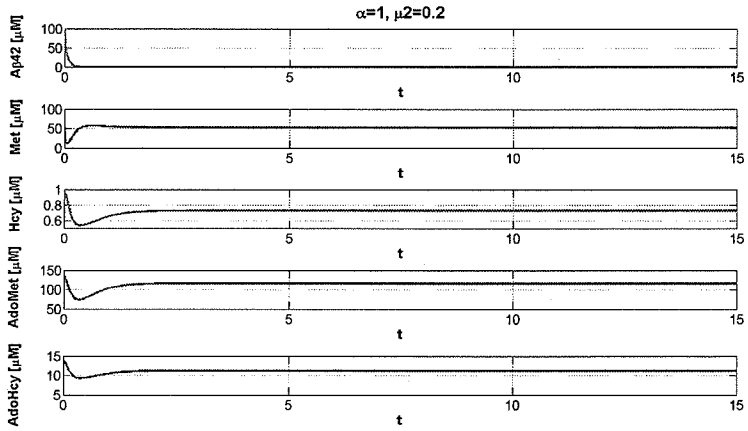

Time series simulations of the 5-compartment model with α=1, μ_2=0.2

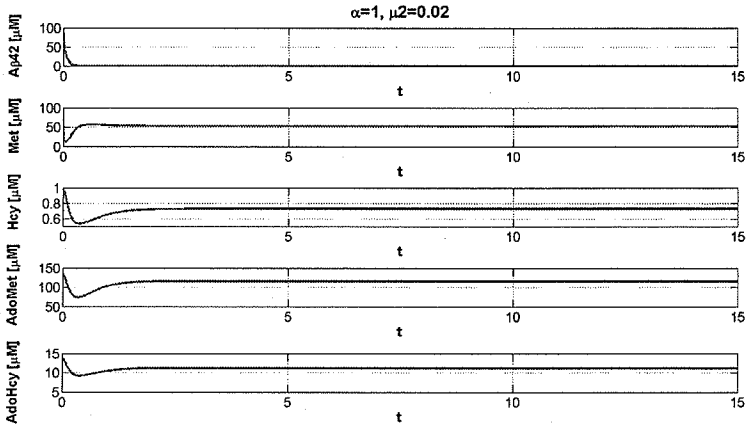

Time series simulations of the 5-compartment model with α=1, μ_2=0.02

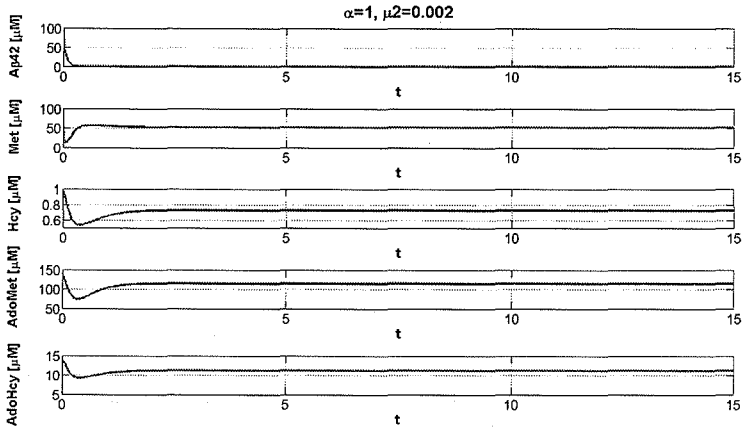

Time series simulations of the 5-compartment model with α=1, μ_2=0.002

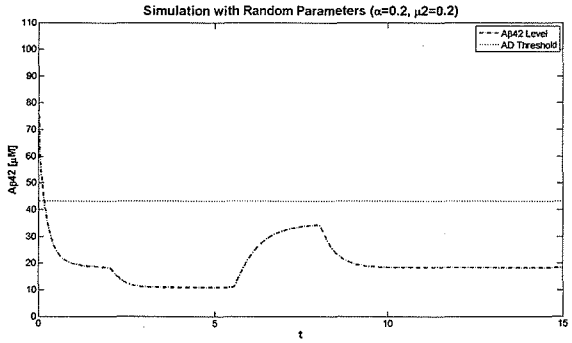

Random Simulation with varied metin and 5mTHF: isolated Aβ_{42} simulation with randomly chosen parameters solely to observe the decay.

During this simulation, and due to constrained data availability, we randomly selected α as 0.5 and μ_2 as 0.2 to observe the decaying behavior of Aβ_{42} concentration. When both α and μ_2 are greater than zero, an overall decay of Aβ_{42} is expected (above). Figure G.2 and Figure G.2 have the same initial decay rate and final steady states. However, Figure G.2 considers both the methionine input (Metin) and the 5mTHF as functions of time. Thus, Figure G.2 illustrated a noticeable fluctuation prior to reaching steady states. In the case of Figure G.2, Metin is fixed at $200\mu M$/h while 5mTHF is fixed at $5.2\mu M$/h. As a result of fixed inputs, Aβ_{42} concentration is a smooth decay, where no fluctuations occur, reaching the steady state earlier in comparison.

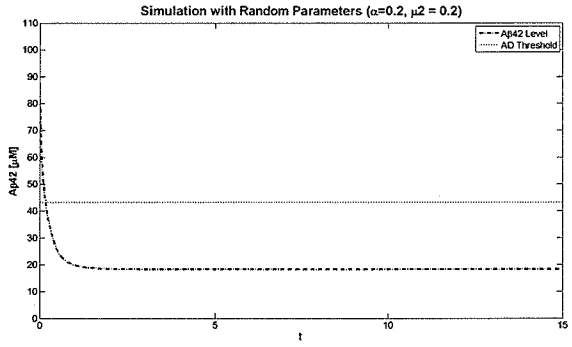

Random Simulation with constant Metin and 5mTHF: this graph serves the same purpose as in Figure G.2 with constants.

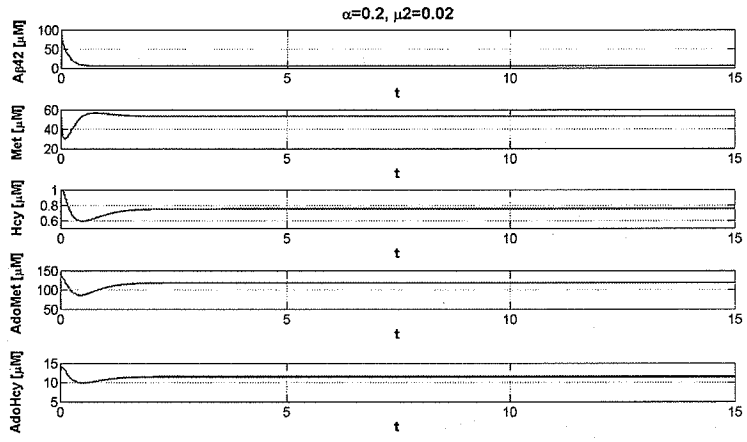

Time series simulations of the 5-compartment model with α=0.2, μ_2=0.02

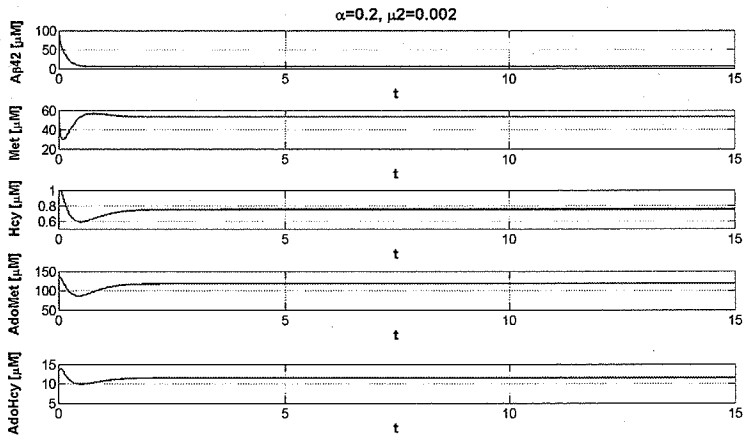

Time series simulations of the 5-compartment model with α=0.2, μ_2=0.002

G.3 MATLAB codes

```
function dy=dydt(t,y) % dydt.m
dy=[0;0;0;0;0];
App=66.5;
mu1=0.76;
alpha= 0.2;
k=200;
p = 87.5/(87.5+k*(87.5-y(1)));

dy(1) = App - mu1*y(1) - alpha*y(2)*y(1);
dy(2) = p*VMS(mTHF(t), y(5)) + p*VBHMT(y(3),y(4),y(5)) + Metin(t) - VMAT1(y(2),y(3))...        - VMAT3(y(2
dy(3) = VMAT1(y(2),y(3)) + VMAT3(y(2),y(3)) - VMETH(y(3),y(4)) - VGNMT(y(3),y(4));
dy(4) = VMETH(y(3),y(4)) + VGNMT(y(3),y(4)) - VAH(y(4),y(5));
dy(5) = VAH(y(4),y(5)) - VCBS(y(3),y(4),y(5)) - p*VMS(mTHF(t),y(5))...
        - p*VBHMT(y(3),y(4),y(5));
end

function run %run.m
close all
clear all
tstart=0;
tstop=15;
y0=[87.5;53.5;137.6;13.2;0.88];
option=odeset('AbsTol',1e-12,'RelTol',1e-9);
[t,y] = ode45('dydt',[tstart;tstop],y0,option);
figure
[AX,H1,H2]=plotyy(t, y(:,1), t, y(:,2),'plot');
xlabel('t')
set(get(AX(1), 'Ylabel'),'String','Abeta42')
set(get(AX(2), 'Ylabel'),'String','Met')
set(H1, 'LineStyle','--')
set(H2, 'LineStyle',':')
legend('Met [microM]','Abeta42 [microM]')
figure
[AY,H3,H4]=plotyy(t, y(:,1), t, y(:,5), 'plot');
xlabel('t')
set(get(AY(1), 'Ylabel'),'String','Abeta42')
set(get(AY(2), 'Ylabel'),'String','Hcy')
set(H3, 'LineStyle','--')
set(H4, 'LineStyle',':')
legend('Hcy [microM]','Abeta42 [microM]')
figure
[AZ,H5,H6]=plotyy(t, y(:,2), t, y(:,5), 'plot');
xlabel('t')
set(get(AZ(1), 'Ylabel'),'String','Met')
set(get(AZ(2), 'Ylabel'),'String','Hcy')
set(H5, 'LineStyle','--')
set(H6, 'LineStyle',':')
legend('Hcy [microM]', 'Met [microM]')
end

function f=Metin(t) % Metin.m
f=200;
% if 0<=t & t<2
% =200;
% else if t>=2 & t<5.5
```

```
% f=300;
% else if t>=5.5 & t<8
% f=100;
% else f=200;
% end
% end
% end
end

function f=mTHF(t) % mTHF.m
f=5.2;
% if 0<=t & t<2
% f=5.2;
% else if t>=2 & t<5.5
% f=7.2;
% else if t>=5.5 & t<8
% f=3.2;
% else f=5.2;
% end
% end
% end
end

function f=VAH(a,b) % VAH.m
 % a :  AdoHcy
%b :  Hcy
alpha1=100;
alpha2=10;

f=alpha1*(a-alpha2*b);

% 100*(SAH- 10*HCY)
end

function f=VBHMT(a,b,c) % VBHM.m
% a :  AdoMet
% b :  AdoHcy
% c :  Hcy
Vbhmtmax=2500;
Kbhmtm=12;

f=(0.7-0.025*(a+b-150))*Vbhmtmax*c/(Kbhmtm+c);

% (0.7-0.025*(AdoMet+AdoHcy-150))*2500*Hcy/(12+Hcy)
end

function f=VCBS(a,b,c) % VCBS.m
% a :  AdoMet
% b :  AdoHcy
% c :  Hcy
beta1=1.7;
beta2=30;

f=(beta1*(a+b)-beta2)*c;

% (1.7*(SAM+SAH)-30)*HCY
```

```
end

function f=VGNMT(a,b) % VGNMT.m
% a :  AdoMet
% b :  AdoHcy
Vgnmtmax=10600;
Kgnmtm=4500;
Kgnmti=20;

f=Vgnmtmax/(1+(Kgnmtm/a)^2.3)*(1/(1+b/Kgnmti));

% 10600/(1+(4500/SAM)^ 2.3)*(1/(1+ SAH/20))
end

function f=VMAT1(a,b) % VMAT1.m
% a :  Met
% b :  AdoMet
Vmat1max=561;
Kmat1m=41;
Kmat1i=50;

f=Vmat1max/(1+Kmat1m/a*(1+b/Kmat1i));

% 561/(1+41/Met * (1+ AdoMet/50))
end

function f=VMAT3(a,b) % VMAT3.m
% a :  Met
%b :  AdoMet
Vmat3max=22870;
Kmat3m1=20000/(1+5.7*(b/(b+600))^2);
Kmat3m2=21.1;

f=Vmat3max/(1+Kmat3m1*Kmat3m2/(a^2+a*Kmat3m2));

% 22870/(1+20000/(1+5.7*(AdoMet/(AdoMet+600))^2)*21.1/(Met^2+Met*21.1))
end

function f=VMETH(a,b) %VMETH.m
% a :  AdoMet
% b :  AdoHcy
Vmethmax=4521;
Kmethm1=1+b/4;
Kmetha=10;

f=Vmethmax/(1+ Kmethm1/a + Kmetha + Kmetha*Kmethm1/a );

% 4521/(1+ (1+SAH/4)/SAM + 10 + 10*(1+ SAH/4)/SAM )
end

function f=VMS(a,b) % VMS.m
% a :  5mTHF
% b :  Hcy
Vmsmax=500;
Kmsmhcy=0.1;
Kmsm5mthf=25;
```

```
Kmsd=1;

f=Vmsmax*a*b/(Kmsd*Kmsmhcy+Kmsmhcy*a+Kmsm5mthf*b+a*b);

%500*5.2*Hcy/(1*0.1+0.1*5.2+ 25*Hcy+5.2*Hcy)
end
```